

Passivation of PEA^+ to $MAPbI_3$ (110) surface states by first-principles calculations

Wei Hu(胡伟), Ying Tian(田颖), Hong-Tao Xue(薛红涛), Wen-Sheng Li(李文生), and Fu-Ling Tang(汤富领)
Citation: Chin. Phys. B, 2021, 30 (**4**): 047101. DOI: 10.1088/1674-1056/abccb7
Journal homepage: http://cpb.iphy.ac.cn; http://iopscience.iop.org/cpb

What follows is a list of articles you may be interested in

Ultra-low Young's modulus and high super-exchange interactions in monolayer CrN: A promising candidate for flexible spintronic applications

Yang Song(宋洋), Yan-Fang Zhang(张艳芳), Jinbo Pan(潘金波), and Shixuan Du(杜世萱)
Chin. Phys. B, 2021, 30 (**4**): 047105. DOI: 10.1088/1674-1056/abdb20

First-principles calculations of F-, Cl-, and N-related defects of amorphous SiO_2 and their impacts on carrier trapping and proton release

Xin Gao(高鑫), Yunliang Yue(乐云亮), Yang Liu(刘杨), and Xu Zuo(左旭)†
Chin. Phys. B, 2021, 30 (**4**): 047104. DOI: 10.1088/1674-1056/abe3f7

Structure prediction, electronic, and mechanical properties of alkali metal MB_{12} (*M*= *Be*, Mg, Ca, Sr) from first principles

Chun-Ying Pu(濮春英), Rong-Mei Yu(于荣梅), Ting Wang(王婷), Zhen-Yan X\"ue(薛振彦), Yong-Sheng Zhu(朱永胜), and Da-Wei Zhou(周大伟)
Chin. Phys. B, 2021, 30 (**1**): 017102. DOI: 10.1088/1674-1056/abb667

Electronic structures, magnetic properties, and martensitic transformation in all-d-metal Heusler-like alloys Cd_2MnTM(*TM*=Fe, Ni, Cu)

Yong Li(李勇), Peng Xu(徐鹏), Xiaoming Zhang(张小明), Guodong Liu(刘国栋), Enke Liu(刘恩克), Lingwei Li(李领伟)
Chin. Phys. B, 2020, 29 (**8**): 087101. DOI: 10.1088/1674-1056/ab9739

Structural, electronic, and magnetic properties of quaternary Heusler CrZrCo*Z* compounds: A first-principles study

Xiao-Ping Wei(魏小平), Tie-Yi Cao(曹铁义), Xiao-Wei Sun(孙小伟), Qiang Gao(高强), Peifeng Gao(高配峰), Zhi-Lei Gao(高治磊), Xiao-Ma Tao(陶小马)
Chin. Phys. B, 2020, 29 (**7**): 077105. DOI: 10.1088/1674-1056/ab969b

---

Passivation of PEA^+ to $MAPbI_3$ (110) surface states by first-principles calculations*

Wei Hu(胡伟)[1,2,3], Ying Tian(田颖)[1,2], Hong-Tao Xue(薛红涛)[1,2], Wen-Sheng Li(李文生)[1,2], and Fu-Ling Tang(汤富领)[1,2,†]

[1] School of Materials Science and Engineering, Lanzhou University of Technology, Lanzhou 730050, China
[2] State Key Laboratory of Advanced Processing and Recycling of Nonferrous Metals, Lanzhou University of Technology, Lanzhou 730050, China
[3] Department of Materials Engineering, Lanzhou Institute of Technology, Lanzhou 730050, China

(Received 6 October 2020; revised manuscript received 10 November 2020; accepted manuscript online 23 November 2020)

The $MAPbI_3$ (110) surface with low indices of crystal face is a stable and highly compatible photosensitive surface. Since the electronic states on the surface can be detrimental to the photovoltaic efficiency of the device, they should be passivated. Phenylethylamine (PEA^+), as a molecular ligand, has been widely used in continuous degradation and interfacial charge recombination experiments, and has satisfactory performance in improving surface defects. Therefore, we construct an adsorption model of $MAPbI_3$ with small molecules, calculating the lattice structure and electronic properties of PEA^+-adsorbed $MAPbI_3$ (110) surface. It is found that PEA^+ as a passivator can effectively weaken the electronic states and regulate the band gap of the $MAPbI_3$ (110) surface. Before and after adding the passivator, the peak value of electronic state densities at $MAPbI_3$ (110) surface is reduced by about 50%, and the band gap is apparently reduced. Moreover, by comparing the Bader atomic charge and spatial charge distributions before and after PEA^+'s adsorption on the surface of $MAPbI_3$, we observe a substantial change of PEA^+ charges, which suggests the surface states have been passivated by PEA^+.

Keywords: first-principles calculations, surface states, passivation

PACS: 71.15.Mb, 31.15.A−, 73.20.−r **DOI:** 10.1088/1674-1056/abccb7

1. Introduction

Although the photoelectric conversion efficiency (PCE) has increased rapidly since the advent of perovskite solar cells (PSCs), researchers are still facing many challenges, such as preparing large-area perovskite films,[1] improving the oxidation stability of the device,[2] and developing effective technology to passivate the surface/interface defects.[3] Besides the properties of each layer material, the surface/interface structures and properties of solar cells are also crucial to the performance, which has led to a recent research focus in pursuing higher conversion efficiency.[4–9] For PSCs, defects of the bulk phase, the grain boundary, and the surface or interface will significantly affect carrier transport and charge recombination, which hinders improving the efficiency of PSCs. In addition, the battery materials prepared under mild conditions are far from the equilibrium state. Thus, there are rich interfaces, structural disorders and defects, which can lead to lower reproducibility of experiments and poor device stability.[10] For this reason, developers try to improve battery performance by modifying and adjusting the surface or interface. Surface states are one of the reasons for low conversion efficiency and poor stability of devices. Therefore, optimizing the passivation method is also a primary way to improve the efficiency and stability of the device. Below, we briefly review some experimental results of perovskite solar cell interface research and regulation. In 2019, You *et al.* summarized the latest progress of effective defect passivation about perovskite solar cells and described in detail the passivation methods of traditional solar cells.[11] For example, two-dimensional perovskite,[12,13] halogen ion,[14] and other materials with wide band gap[15] are commonly used to passivate surface defects. Moreover, the national renewable energy laboratory (NREL) also introduced the necessity of passivation of bulk or surface (interface) defects by additives and summarized the performances of additives used to control surface defects of perovskite, such as metal cations, fullerene derivatives, ammonium salts, low dimensional perovskite.[16,17] Abdi-Jalebi *et al.* found that when KI was added to the perovskite precursor, K^+ would accumulate on the surface to passivate those expanding defects; thus, the perovskite film with PCE of 21.5% could be produced.[18] Lee *et al.* reported the advantages of adding PEA^+ into 3D perovskite, and the wide band gap quasi-2D perovskite based on PEA^+ is conducive to reducing the defect density and slowing down the degradation of the unpacked devices.[19] Compared with the traditional 3D perovskite, the low-dimensional perovskite with 2D layered structure has better phase stability due to its large organic cation; in addi-

*Project supported by the National Natural Science Foundation of China (Grant Nos. 11764027 and 51674130), the Scientific Research Projects of Higher Education in Gansu Province, China (Grant No. 2018A-126), and the Research Team Support Program of Lanzhou Institute of Technology (Grant Nos. 2018KW-11 and 2020KJ-01).

†Corresponding author. E-mail: tfl@lut.edu.cn

© 2021 Chinese Physical Society and IOP Publishing Ltd

tion, the hydrophobic effect of phenyl makes the device have better moisture resistance.[20,21] Among low-dimensional perovskites, the passivation effect of phenethylammonium iodide (PEAI) is most commendable,[22–24] probably due to the more ordered 2D passivation layer formed by PEAI, and the synergistic effect of three groups is conducive to the longitudinal transport.[25] Based on this, the first principle calculation method based on density functional theory is used to study the passivation effect of PEA^+ on the electronic states of $MAPbI_3$ (110) surface.

2. Methods and model

In this work, all the calculations are performed with the code package VASP based on the density functional theory (DFT).[26,27] The exchange–correlation energy is described by the functional of Perdew–Burke–Ernzerh (PBE) [28] in the generalized gradient approximation (GGA), and the pseudopotential is described by projector-augmented wave (PAW).[29] By cutting the bulk $MAPbI_3$ along the (110) direction, when surface termination is MA^+ cation (as shown in Fig. 1), the system contains 6 periodic atomic layers (excluding pseudo-H layer) of A-B, and the structure of the model is complete. In order to make the PEA^+ cations play an effective passivation role on this surface, I is made the surface terminal atom, and the top A-layer1 is deleted. The model forms a symmetrical nonpolar surface of the upper and lower atomic layers. PEA^+ is placed on the exposed and clean $MAPbI_3$ (110) surface with B-layer2 to establish the adsorption model. The passivation of H atom is added to eliminate the influence of the surface hanging bond of the bottom atom. The adsorption system consists of 84 atoms (43 H, 6 N, 13 C, 17 I, and 5 Pb). The electronic configurations of Pb, I, N, C and H atoms in the crystal model are [Xe] $5d^{10}6s^26p^2$, [Kr] $4d^{10}5s^25p^5$, C $2s^22p^2$, N $2s^22p^3$ and $1s^1$, respectively. The cutoff energy of $MAPbI_3$ surface and its adsorption system is 520 eV, and the k-point grids of the Brillouin region are set to $6 \times 4 \times 1$. We use the conjugate gradient algorithm to optimize the original structure of the clean surface and the adsorption model. The convergence condition of the atomic force is set to 5×10^{-2} eV/Å. Then, the adsorption energy and density of states (DOS) of the model are calculated according to the Bloch tetrahedron method.

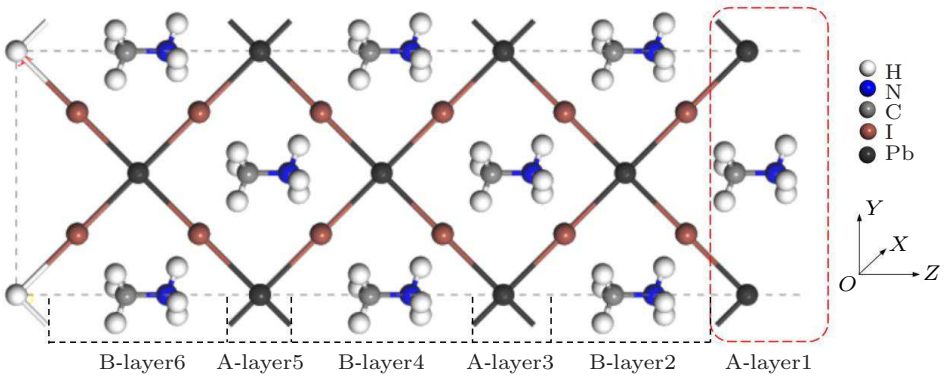


Fig. 1. Atomic terminal of $MAPbI_3$ (110) surface model.

3. Results and discussion

3.1. Lattice structure and electronic properties of clean $MAPbI_3$ (110) surface

In order to effectively analyze the passivation effect of PEA^+, the electronic properties of clean $MAPbI_3$ (110) surface model are calculated. The $MAPbI_3$ (110) surface model of six atomic layers (including 31 H, 5 N, 5 C, 17 I, and 5 Pb atoms) is constructed (including pseudo-H layer). The lattice constants are $a = 6.330$ Å, $b = 8.952$ Å, $c = 23.283$ Å. In addition, a 20 Å thickness vacuum layer is added along the Z axis to avoid the influence of periodic images of atoms. During the relaxation process, the top 2 layers of $MAPbI_3$ (110) surface model are fully relaxed, and the bottom 4 layers atoms (including pseudo-H layer) far away from the surface are fixed to simulate the bulk. Figure 2 shows the optimized structure of $MAPbI_3$ (110) surface model, in which the first two layers close to the surface are released, and the third to fifth layers are fixed to simulate the bulk. After calculation, it is found that the atoms positions shift, and the bond lengths (angles) of certain atoms have changed. In the first layer, I atoms of the surface move along the Y axis, and the distance of the two atoms increases from 4.476 Å to 4.767 Å. For I atoms far away from the surface, they are close to the center along the Y axis, and the distance reduces from 4.476 Å to 4.128 Å. The average bond length $d_{Pb–I}$ is 3.1855 Å along the X axis, and the bond length $d_{Pb–I}$ of bulk $MAPbI_3$ is 3.165 Å, which shows that the bond length extends, and I and Pb atoms move up along the Z axis with the distances of 0.333 Å and 0.031 Å, respectively. The whole organic MA^+ cation moves down by 0.039 Å along the Z axis, and the C–N bond length decreases

slightly, and the angle H–C–H of CH_3 ion increases by 1.036°. However, the angle H–N–H of NH_3 ion decreases by 2.966°. For the second layer, the bond lengths d_{Pb-I} are 3.196 Å and 3.169 Å on the X axis, respectively. The bond length has increased compared with that of before structural optimization. I atom moves up 0.298 Å along the Z-axis direction, while Pb atom moves 0.027 Å in the opposite direction. Affected by the upper atoms, the whole organic MA^+ cation moves down 0.052 Å along the Z-axis, and the bond length d_{C-N} decreases from 1.510 Å to 1.497 Å, and the angle H–C–H of CH_3 ion increases by 1.259°, while the angle H–N–H of NH_3 ion decreases by 3.234°. Through the above analysis, it is found that the average bond length of d_{Pb-I} increase by 0.039 Å, which is much larger than the average bond length change of d_{Pb-I} (0.017 Å) in the second layer. In the first layer, the I and Pb atoms move more along the Z-axis, while the I and Pb atoms move less in the second layer. This shows that the extension (or contraction) of bond lengths mainly occurs in the first layer near the surface. That is to say, the change of bond length is more obvious for those closer to the surface; the atoms will move a greater distance under a greater influence from the surface such that a more stable equilibrium position will be reached in the relaxation process.

Figure 3 shows the total density of states (TDOS) of clean $MAPbI_3$ (110) surface, and the local density of states (LDOS) of each layer, and the partial density of states (PDOS) of some atoms on the surface. From the TDOS (Fig. 3(a)), it can be found that there is a peak near the Fermi level between −1 eV and −0.5 eV, and DOS is 11.5 at the Fermi level, which indicates the existence of electronic states. According to Figs. 3(b)–3(f), it can be found that these electronic states mainly come from the first, the third, and the fifth layer of atoms. From Figs. 3(g)–3(j), the peak of density of states is mainly contributed by the I-5p, Pb-6s, and Pb-6p orbitals on the first layer of the surface near the Fermi level. These electronic states are surface states, which may have harmful effects on the surface. The main reason is that the existence of the electronic states leads to the radiation compound loss of the photo-generated carriers on the surface, which reduces the PCE of devices. Therefore, it is particularly important to find the surface passivators to weaken or even eliminate the electronic states.

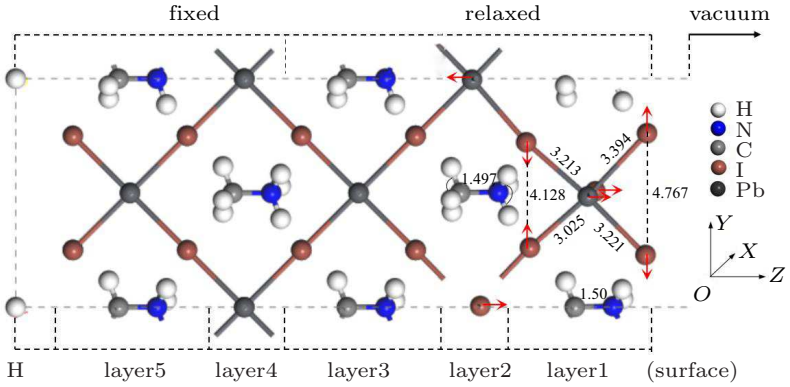


Fig. 2. The optimized atomic position change of clean $MAPbI_3$ (110) surface.

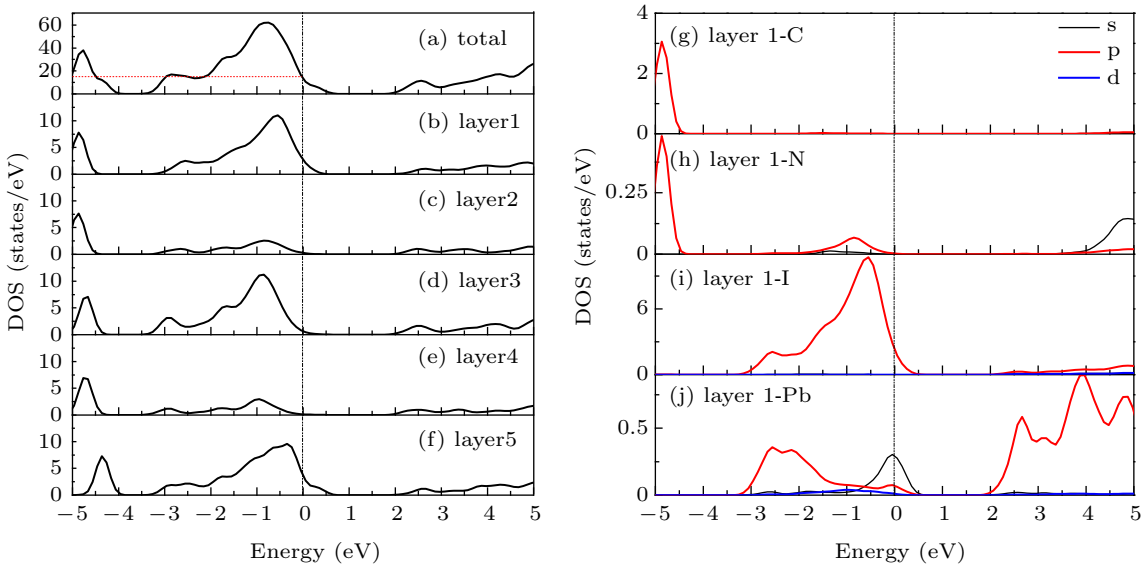


Fig. 3. (a) The TDOS of clean $MAPbI_3$ (110) surface; (b)–(f) the LDOS of layer1–layer5; (g)–(j) the PDOS of layer1.

3.2. Adsorption structure of PEA^+-$MAPbI_3$

According to the literature research, the passivator PEA^+ has been widely studied for its excellent passivation performance,[19,22] so we use it to treat the electronic states of $MAPbI_3$ (110) surface. The single point energy calculation is used to obtain the optimal adsorption distance from the passivator to the surface (the head and tail of passivator to the surface are calculated respectively), and the adsorption structure is determined by the lowest energy of the system. The relationship between the adsorption distance and the total energy is shown in Fig. 4. The calculations confirm that when PEA^+ is 3.393 Å away from the $MAPbI_3$ (110) surface, the total energy of the whole system is the lowest (−389.377 eV).

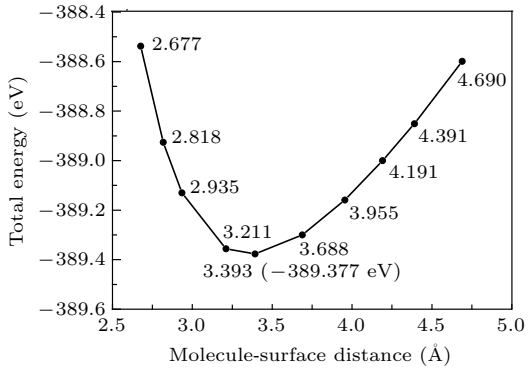


Fig. 4. Total energy of the PEA^+ system in different adsorption distance.

Figure 5 shows the surface adsorption model, which contains 84 atoms. In order to eliminate the influence of the surface atom hanging bond, passivated H atoms are added to the left of the model. In order to avoid the interaction of periodic atoms, a 10 Å vacuum layer is added. In the process of optimizing the model, the first and the second layer atoms of $MAPbI_3$ (110) surface and PEA^+ are released, and the remaining layers far away from the $MAPbI_3$ (110) surface are fixed. The red arrow is used to indicate the moving direction of the atom after the relaxation of the adsorption structure in Fig. 5. On the first layer, the I atoms are close to the center along the Y axis near the adsorption surface, while the I atoms move in the opposite direction far away from the surface. The variation values are as follows: the former decreases by 0.204 Å, the latter increases by 0.022 Å. The average bond length $d_{Pb–I}$ is 3.212 Å on the Y–Z plane. I and Pb atoms move 0.354 Å and 0.051 Å in the positive and negative directions respectively along the Z axis, and the bond lengths $d_{Pb–I}$ are 3.179 Å and 3.160 Å respectively, which are 0.007 Å and 0.025 Å shorter than that of before optimization. Compared with the optimized structure of the clean surface, these I atoms move in the opposite direction, which is related to the adsorption passivator on the surface. MA^+ cations move up slightly along the Z-axis, in which C–N bond length, H–C–H bond angle, and H–N–H bond angle change little. In the second layer, Pb and I atoms move 0.008 Å and 0.057 Å in the positive and negative directions along the Z axis, respectively. The average bond length $d_{Pb–I}$ is 3.1755 Å. The downward movement distance of MA^+ cations along the Z axis is larger than the upward movement distance of MA^+ cations of the first layer, and the changes of bond length and bond angle of each component are larger than that of the first layer. After the adsorption system relaxation, the bond length (angle) of PEA^+ also has a change in different degrees. The most obvious is that the C–N bond length increases by 0.018 Å near the surface, and the N–C–C bond angle increases by 2.078°. From the above analysis, it can be seen that the Pb, I atoms, and MA^+ cations of the center position will move greatly due to the adsorption of the passivator PEA^+. Due to the periodic destruction of the lattice structure near the surface, the change of the atoms closer to the surface is more obvious in the relaxation process.

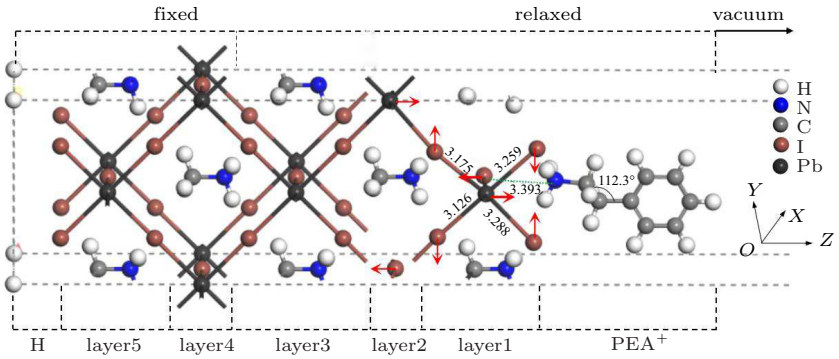


Fig. 5. The change of atom position in the optimized adsorption system.

3.3. Adsorption energy and electronic properties of PEA^+-$MAPbI_3$ adsorption system

The stability of surface adsorption is related to the adsorption energy of the system. In other words, if the adsorption energy is negative, the smaller the value, the more stable the adsorption of molecules or atoms on the surface.[30] Equation (1) is used to calculate the adsorption energy of PEA^+ on $MAPbI_3$ (110) surface[31]

$$E = [E_{\text{atom/MAPbI}_3} - E_{\text{MAPbI}_3} - NE_{\text{atom}}]/N. \quad (1)$$

$E_{\text{atom/MAPbI}_3}$ and E_{MAPbI_3} represent the total energy of adsorption system and clean surface $MAPbI_3$ (110), respectively. E_{atom} is the total energy of the adsorbate PEA^+. N is 1, which means to adsorb a molecule. The adsorption energy of the system is −3.898 eV. The result shows that the system has higher absorbability, and it also shows that the passivator has good stability on this surface.

Surface states (electronic states) are an unfavorable factor for solar cells. It serves as a carrier recombination center for photogenerated carriers and will thereby reduce the carrier lifetime as well as PCE. Compared Fig. 3 with Fig. 6, the passivation effect of PEA^+ on the $MAPbI_3$ (110) surface can be analyzed. It can be seen that the passivator PEA^+ greatly reduces the electronic states of $MAPbI_3$ surface, and its value of total DOS decreases from 11.5 to 6.5 at the Fermi level. Thus, PEA^+ treatment should greatly suppress trap-assisted charge recombination and improve PCE. This is basically consistent with the experimental results of Zhang *et al.*[22–24] Through the analysis of the PDOS, it may be seen that the decrease of the electronic states peak value is mainly due to the contribution of I-5p and Pb-6p, Pb-6s on the first layer of $MAPbI_3$ (110) surface near the Fermi level within −1.5 to 0.3 eV. Moreover, compared with the band gap of clean $MAPbI_3$ (110) surface, the band gap of the adsorption system decreases significantly, and it also shows that PEA^+ can regulate the band gap of $MAPbI_3$ (110) surface. Figure 6(b) shows that the adsorption of PEA^+ does not introduce new electronic states, which has a good passivation effect. Compared with the local density of states of clean $MAPbI_3$ (110) surfaces (Figs. 5(b)–5(e)), it can be seen that the first four layers have no DOS peak due to the addition of passivator near the Fermi level. In particular, the passivation effect of PEA^+ on the first and third layers is most obvious in Figs. 6(c)–6(f). Figures 6(i)–6(n) show the PDOS of C, N, I, and Pb atoms at the adsorption surfaces of $MAPbI_3/PEA^+$. According to Figs. 6(i), 6(l) and 6(n), there is hybridization of C-2p orbital of PEA^+ and N-2s with the Pb-6p orbital of $MAPbI_3$ near the Fermi level within 1.5 to 2.5 eV. Figures 6(i) and 6(m) show that there is a hybridization of C-2p orbital of PEA^+ and I-5p orbital of $MAPbI_3$. According to the above analysis, the adsorption of PEA^+ on the $MAPbI_3$ (110) surface has a good passivation effect, and the electronic orbital hybridization also promotes interaction between atoms.

Charge density difference and Bader charge are qualitative and quantitatively described of the surface charge transfer degree, respectively. By calculating the charge density difference and Bader charge, we can fully understand the charge transfer of the whole system.[32] Charge density difference is calculated by

$$\Delta\rho = \rho_{\text{atom/MAPbI}_3} - \rho_{\text{MAPbI}_3} - \rho_{\text{atom}}. \quad (2)$$

Here, $\rho_{\text{atom/MAPbI}_3}$ represents the total charge density of the adsorption system, ρ_{MAPbI_3} and ρ_{atom} respectively represent the independent charge density values of $MAPbI_3$ and PEA^+ in the same adsorption system.

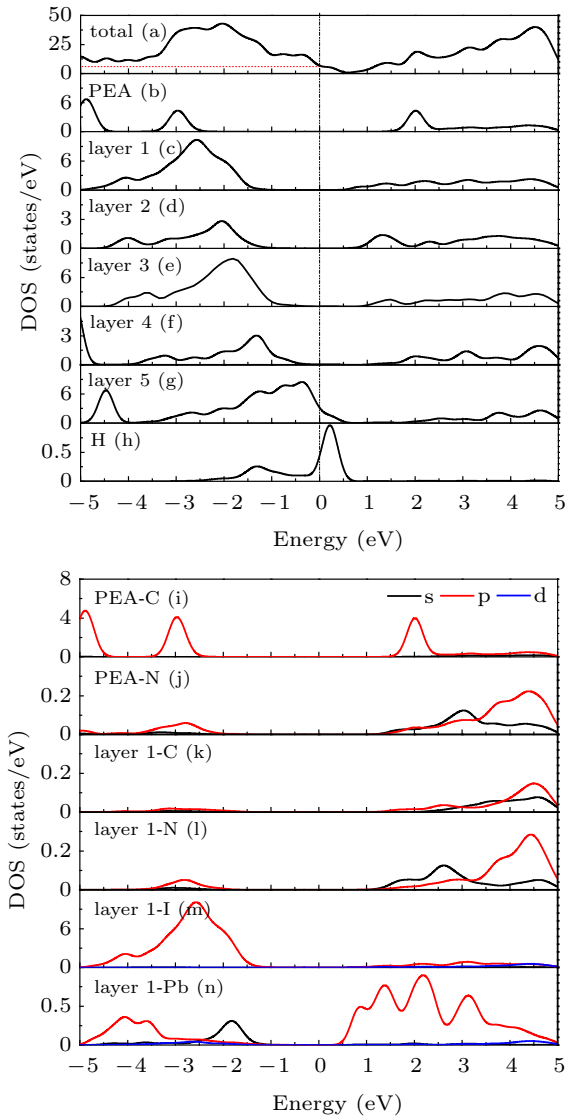


Fig. 6. (a) The TDOS of PEA^+-$MAPbI_3$ adsorption system; (b) the LDOS of PEA^+; (c)–(g) the LDOS of layer1–layer5; (h) the LDOS of passivation H; (i)–(n) the PDOS of PEA^+ and $MAPbI_3$ (110) layer1.

Figure 7 shows the charge density difference of PEA^+ adsorbed on the surface of $MAPbI_3$ (110). The increase (positive) or decrease (negative) of charge density is indicated by yellow and cyan, respectively. Figure 7(a) is the charge density difference of the adsorption system, and Fig. 7(b) is a partially enlarged diagram of the charge density difference of the adsorption system. From Fig. 7(a), it can be seen that the charge transfer takes place throughout the system but mainly concentrates near the surface; the farther from the surface, the smaller the charge transfer. The charge density difference culminates on the surface, and the charge transfers are directed to both sides of the surface, which will promote the bonding strength between the surface atoms, leading to strong atoms interaction on the surface. From Fig. 7(b), it can be seen that I atoms gain electrons, and Pb atoms lose electrons. For the PEA^+ part, the

number of C atoms electron is reduced while the number of N atom electron increases near the surface.

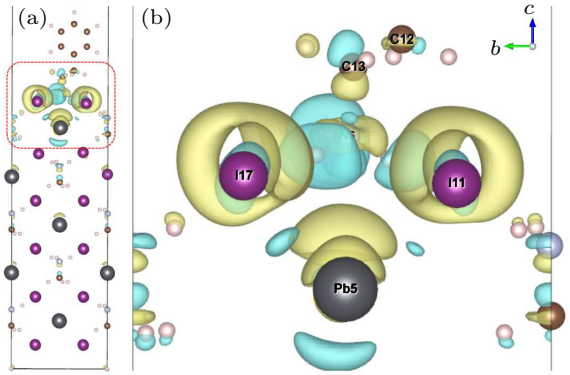


Fig. 7. Density charge difference of the PEA^+-$MAPbI_3$ adsorption system.

The amount of charge transfer is analyzed by calculating the Bader charge of each atom of the adsorption structure surface and bulk phase. Table 1 shows the Bader charges of I, Pb, C, N atoms of $MAPbI_3$ and PEA^+ bulk, and that of the adsorption system near the surface. It can be found that I5, I11, and I17 atoms get 0.588*e*, 0.669*e*, and 0.684*e*, respectively, while Pb5 atom loses 0.892*e* on the first layer of adsorption system $MAPbI_3$. Compared with the Bader charge of I and Pb atoms in the original phase, I and Pb atoms of the adsorption system gain or lose more electrons. Compared Bader charge of the adsorption system PEA^+ with that of the independent system PEA^+, it can be seen that N atom gets 2.944*e*, C12 atom gets 0.779*e*, and C13 loses 0.523*e* near the adsorption system surface. To sum up, through the analysis of Figs. 6 and 7, combined with Bader charge, it can be seen that the decrease of the surface states of $MAPbI_3$ (110) is mainly due to the contribution of C and N atoms of passivator PEA^+. The above results show that the Bader charge changes greatly before and after PEA^+ adsorbed on the $MAPbI_3$ surface, which indicates that the surface chemical reaction is strong. On the other hand, it can be seen that the farther away from the surface, the smaller the charge transfer.

Table 1. Bader charges of some atoms of $MAPbI_3$ bulk and PEA^+-$MAPbI_3$ adsorption system.

Systems	I	Pb	C	N
Bulk of $MAPbI_3$	$-0.50 \sim -0.49$	0.73		
$MAPbI_3$ layer1	$-0.68 \sim -0.59$	0.89		
PEA^+			$0.02 \sim 0.23$	-1.13
PEA^+ on surface			$-0.78 \sim 0.52$	-2.94

4. Conclusion

In this work, the passivation effect of PEA^+ to the electronic states of $MAPbI_3$ (110) surface is studied using VASP software based on the first principle calculations. The results show that surface electrons are redistributed and the surface states are passivated. The C and N atoms of the passivator PEA^+ surface can eliminate the surface states, which is mainly due to the contribution of I-5p and Pb-6p, Pb-6s on the first and the third layer of $MAPbI_3$ (110) surface near the Fermi level between -1.5 eV and 0.3 eV by adding the passivator. The study of passivated surface provides a theoretical guideline for enhancing the transmission of photogenerated carriers and is inspiring to improve the PCE of $MAPbI_3$-based solar cells.

Acknowledgment

This work was performed in the Gansu Supercomputer Center.

References

[1] Luo L, Zhang Y, Chai N, Deng X, Zhong J, Huang F, Peng Y, Cheng Y B and Ku Z 2018 *J. Mater. Chem. A* **6** 21143
[2] Zhang L and Sit P H L 2016 *RSC Adv.* **6** 76938
[3] Wang S, Zhu Y, Wang C and Ma R 2019 *J. Mater. Chem. A* **7** 11867
[4] Zhou H, Chen Q, Li G, Luo S, Song T, Duan H S, Hong Z, You J, Liu Y and Yang Y 2014 *Science* **345** 542
[5] Shi J, Xu X, Li D and Meng Q 2015 *Small* **11** 2472
[6] Graetzel M, Janssen R A, Mitzi D B and Sargent E H 2012 *Nature* **488** 304
[7] Ding S, Li S, Sun Q, Wu Y C, Liu Y, Li Z, Cui Y, Wang H, Hao Y and Wu Y 2019 *J. Mater. Chem. C* **7** 5686
[8] Shi S, Gao J, Liu Y, Zhao Y, Wu Q, Ju W, Ouyang C and Xiao R 2016 *Chin. Phys. B* **25** 018212
[9] Gao J, Shi S and Li H 2016 *Chin. Phys. B* **1** 18210
[10] Shi J, Xu X, Li D and Meng Q 2015 *Small* **11** 2472
[11] Gao F, Zhao Y, Zhang X and You J 2019 *Adv. Energy Mater.* **10** 1902650
[12] Hu Y, Schlipf J, Wussler M, Petrus M L, Jaegermann W, Bein T, Mullerbuschschbaum P and Docampo P 2016 *ACS Nano* **10** 5999
[13] Bai Y, Xiao S, Hu C, Zhang T, Meng X, Lin H, Yang Y and Yang S 2017 *Adv. Energy Mater.* **7** 1701038
[14] Yantara N, Yanan F, Shi C, Dewi H A, Boix P P, Mhaisalkar S G and Mathews N 2015 *Chem. Mater.* **27** 2309
[15] Koushik D, Verhees W, Kuang Y, Veenstra S, Zhang D, Verheijen M A, Creatore M and Schropp R E I 2017 *Energy Environ. Sci.* **10** 91
[16] Zhang F and Zhu K 2019 *Adv. Energy Mater.* **10** 1902579
[17] Kim M, Kim G, Lee T K, Choi I W, Choi H W, Jo Y, Yoo Y J, Kim J W, Lee J, Huh D, Lee H, Kwak S K, Kim J Y and Kim D S 2019 *Joule* **3** 2179
[18] Abdijalebi M, Andajigarmaroudi Z, Cacovich S, Stavrakas C, Philippe B, Richter, J M, Alsari M, Booker E P, Hutter E M, Pearson A J, Lilliu S, Savenije T J, Rensmo H, Divitini G, Ducati C, Friend R H and Stranks S D 2018 *Nature* **555** 497
[19] Lee D S, Yun J S, Kim J, Soufiani A M, Chen S, Cho Y, Deng J S, Lim S, Huang S and Hobaillie A 2018 *ACS Energy Lett.* **3** 647
[20] Li N, Zhu Z, Dong Q, Li J, Yang Z, Chueh C, Jen A K Y and Wang L 2017 *Adv. Mater. Interfaces* **4** 1700598
[21] Kim H, Lee Y H, Lyu T, Yoo J H and Oh J H 2018 *J. Mater. Chem. A* **6** 18173
[22] Zhang F, Huang Q, Song J, Zhang Y, Ding C, Liu F, Liu D, Li X, Yasuda H, Yoshida K, Qu J, Hayase S, Toyoda T, Minemoto T and Shen Q 2020 *Solar RRL* **4** 1900243
[23] Jiang Q, Zhao Y, Zhang X, Yang X, Chen Y, Chu Z, Ye Q, Li X, Yin Z and You J 2019 *Nat. Photon.* **13** 460
[24] Xu C, Zhang Z, Hu Y, Sheng Y, Jiang P, Han H and Zhang J 2018 *J. Energy Chem.* **27** 764
[25] Lee K, Kim J, Yu H, Lee J W, Yoon C, Kim S K and Jang J 2018 *J. Mater. Chem. A* **6** 24560
[26] Kresse G and Furthmüller J 1996 *Comput. Mater. Sci.* **6** 15
[27] Kresse G and Furthmüller J 1996 *Phys. Rev. B* **54** 11169
[28] Perdew J P, Burke K and Ernzerhof M 1996 *Phys. Rev. Lett.* **77** 3865
[29] Kresse G and Joubert D 1999 *Phys. Rev. B* **59** 1758
[30] Wen Z, Zhao Y, Hou H, Wang N, Li F U and Han P 2014 *T. Nonferr. Metal. Soc.* **24** 1500
[31] Li D F, Zu X T, Xiao H Y and Liu K Z 2009 *J. Alloy. Compd.* **467** 557
[32] Wang C, Gao H, Dai Y, Ruan X, Shen J, Wang J and Sun B 2010 *J. Alloy. Compd.* **490** L9